Inaccessible time to visual awareness during attentional blinks in macaques and humans

AUTHOR(S):

Chinen, Koji; Kawabata, Akira; Tanaka, Hitoshi; Komura, Yutaka

CITATION:

Chinen, Koji ...[et al]. Inaccessible time to visual awareness during attentional blinks in macaques and humans. iScience 2023, 26(11): 108208.

ISSUE DATE:

2023-11-17

URL:

http://hdl.handle.net/2433/286130

iScience

CellPress OPEN ACCESS

Article

Inaccessible time to visual awareness during attentional blinks in macaques and humans

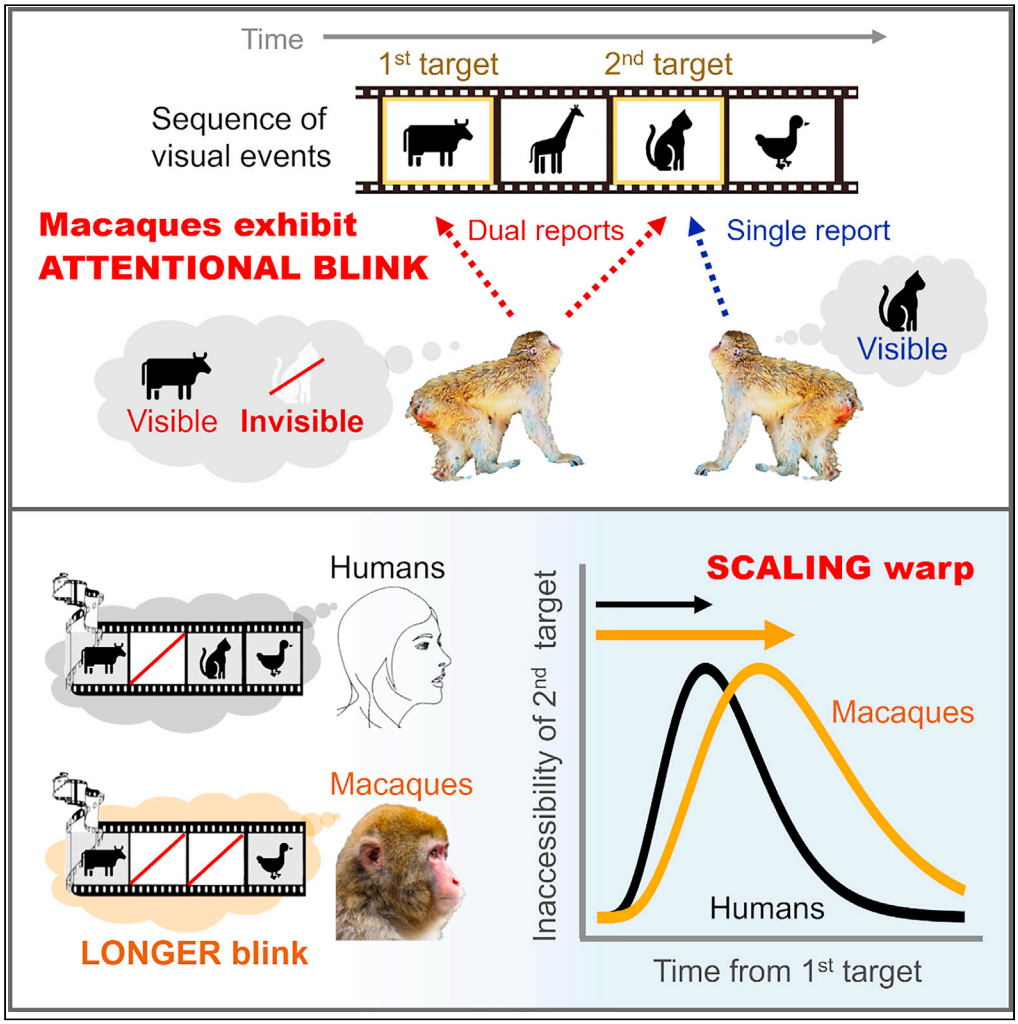

Koji Chinen, Akira Kawabata, Hitoshi Tanaka, Yutaka Komura

komura.yutaka.6a@kyoto-u.ac.jp

Highlights

Attentional blink, a marker of temporal blind spot in awareness, exists in macaques

Macaques exhibit longer attentional blink than humans

Time warping analysis revealed a formal structure behind the interspecies difference

Both primates likely share a scale-invariant mechanism for visual awareness

Chinen et al., iScience 26, 108208
November 17, 2023
https://doi.org/10.1016/j.isci.2023.108208

iScience

CellPress OPEN ACCESS

Article

Inaccessible time to visual awareness during attentional blinks in macaques and humans

Koji Chinen,[1] Akira Kawabata,[1] Hitoshi Tanaka,[1] and Yutaka Komura[1,2,*]

SUMMARY

Even when we attend to successive visual events, we often cannot notice an event occurring during a certain temporal window. Such an inaccessible time for visual awareness is known as "attentional blink" (AB). Whether AB is a phenomenon unique to humans or exists also in other animals is unclear. Using a dual-task paradigm shared between macaques and humans, we here demonstrate a nonhuman primate model of AB. Although macaques also showed behavioral signatures of AB, their AB effect lasted longer than that of humans. To map the relation between macaque and human ABs, we introduced a time warping analysis. The analysis revealed a formal structure behind the interspecies difference of AB; the temporal window of macaque AB was scaled from that of human AB. The present study opens the door to combining the approaches of neuroscience, psychophysics, and theoretical models to further identify a scale-invariant biological substrate of visual awareness.

INTRODUCTION

When people must report two visual targets presented in a rapid serial presentation, the ability to identify the second target is impaired if it is presented within several hundreds of milliseconds from the first target. This phenomenon is known as attentional blink (AB),[1–4] which has provided an important opportunity to study the temporal (in)accessibility to visual awareness in humans.[5,6] However, it has been difficult to elucidate whether AB also occurs in nonhuman animals. The first reason is that most studies testing perceptual behaviors of animals have relied on single reports.[7,8] The second reason is that the previous AB studies in humans have often used characters such as numbers and letters,[1–4] which are unsuitable for an animal's task. In this study, we replaced a sequence of characters with simple shapes and developed a dual-task paradigm applicable to both macaques and humans (STAR Methods). Such a shared experimental design for macaques and humans enables us to test the existence of AB in macaques and to directly compare the psychometric functions from both primate species.

In the previous human studies, various types of AB modifications have been reported, depending on individual experimental[9,10] and clinical conditions[11–13] including neurological and mental disorders. However, a quantitative method for evaluating the AB modifications has not been established. This is because the psychometric function of AB shows an asymmetric U-shaped curve, which it is difficult to parametrize based on a theoretical framework. AB is often explained by a two-stage theory of perception, where the early stage of parallel sensory processing is followed by the late stage of serial processing under limited attentional resources.[1–6] Both the first target (T1) and the second target (T2) can be processed at the early stage; however, while the T1 process is percolated at the late stage, the T2 process is prevented from the late stage, leading to unawareness of T2. In order to characterize AB modifications quantitatively, we incorporated the two-stage model to a time warping method.[14–16] This method is useful for comparing two temporal sequences; the difference can be quantified by a warping function which transforms one sequence to fit another sequence. Using time warping modeling, the present study succeeded in formulating the relation between ABs of macaques and humans.

RESULTS

Attentional blink exists in macaques

We first conducted experiments on two macaques. In the experimental paradigm, the stimulus sequence contained two targets and masks. The first target (T1) was a sinusoidal grating with horizontal or vertical orientation, and the second target (T2) was a white disk, which was followed by two masks (Figure 1A). The task condition is an important variable in AB; the present study included a single task and a dual task. The single task required subjects only to detect T2. The dual task required subjects to discriminate the orientation of T1 in addition to detecting T2 (Figure 1B). The stimulus onset asynchrony (SOA) between T1 and T2, another critical variable in AB, was set to a range from 50 to 850 ms. To clarify the extent to which attention to T1 influences T2 detection, we compared the correct ratio of a subject's

[1]Graduate School of Human and Environmental Studies, Kyoto University, Yoshida-Nihonmatsu-cho, Sakyo-ku, Kyoto 606-8501, Japan
[2]Lead contact
*Correspondence: komura.yutaka.6a@kyoto-u.ac.jp
https://doi.org/10.1016/j.isci.2023.108208

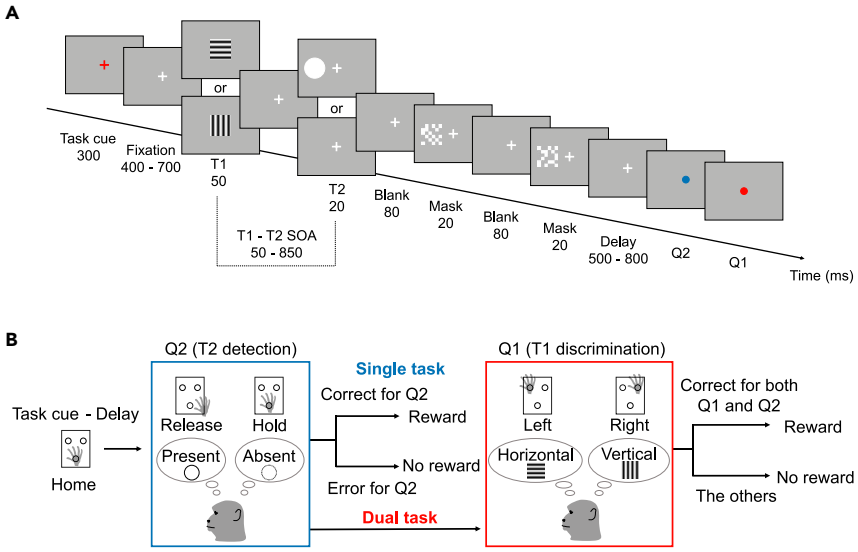

Figure 1. Shared paradigm for testing attentional blink in macaques and humans

(A) Stimulus sequence in the dual task. In each trial, two targets were briefly presented. A horizontal or vertical grating (T1) was presented at the center of the display. A white disk (T2) was flashed at the left parafoveal location in one-half of all trials, followed by two masks. In the other one-half of trials, T2 was absent. Both macaques and humans performed either the single or dual task, per block: the single task only for T2 detection, or the dual task both for T1 orientation discrimination and T2 detection. The colored fixation cross at the beginning of the trial signaled to subjects which task was to be performed: blue for the single task or red for the dual task. The stimulus onset asynchrony between T1 and T2 (i.e., the T1–T2 SOA) varied from 50 to 850 ms on a trial-by-trial basis. For the clarity of illustration, the sizes of T1, T2 and mask stimuli are shown larger than their actual sizes (See STAR Methods).

(B) Stimulus-response associations for macaques. During the Q2 period for T2 detection, macaques had to continue to grip the bar if T2 was absent and release the bar and re-grip it if T2 was present. During the Q1 period for T1 discrimination, macaques were required to touch the upper-left bar if T1 was horizontal or the upper-right bar if T1 was vertical. In the single task, macaques were given a liquid reward after they correctly performed T2 detection. In the dual task, macaques were given a reward only if they correctly performed both T2 detection and T1 discrimination. In the case of the human experiments, the participants reported T1 and T2 by clicks on a PC mouse instead of bar responses.

performance for T2 (T2 accuracy) in the single and dual tasks. In accordance with previous studies of AB in humans,[1–4] T2 accuracy in the dual task was evaluated by the ratio of the correct T2 performance conditional on correct T1 performance. The T2 accuracy of the dual task for both macaques exhibited U-shaped patterns as a function of the T1–T2 SOA (Figures 2A and S1, see also Figure S2 for the signal detection theory measures), as typically observed in previous studies on humans' AB.[1–4] To examine which SOAs significantly differed in T2 accuracy between the single and dual task, we performed *t*-tests with Bonferroni corrections. The results revealed significantly lower T2 accuracy in the dual task than in the single task for 50–700 ms of SOA ($p < 0.01$; see Table S1 for statistics). In the classical studies of human AB, incorrect ratios of T2 detection were often reported to be reduced when T2 was presented immediately after T1. This phenomenon is known as lag-1 sparing,[17,18] but is not always necessary for evidence of AB. To statistically examine the existence of lag-1 sparing in macaques, we compared the T2

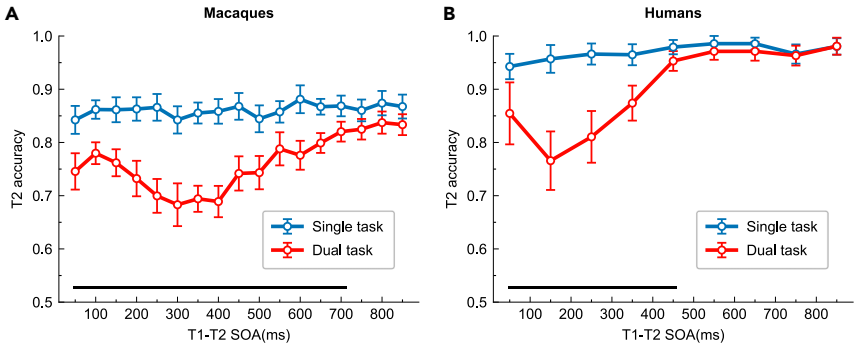

Figure 2. Attentional blink in macaques and humans

(A and B) The means of T2 accuracy in macaques (A) and humans (B). Blue and red lines are the results of single- and dual-task conditions, respectively. Error bars represent 95% confidence intervals of mean. Horizontal bars at the top of the x axis indicate SOAs at which significant differences were obtained between both task conditions ($p < 0.05$, t-tests with the Bonferroni method). See also Figures S1 and S2, Tables S1 and S2.

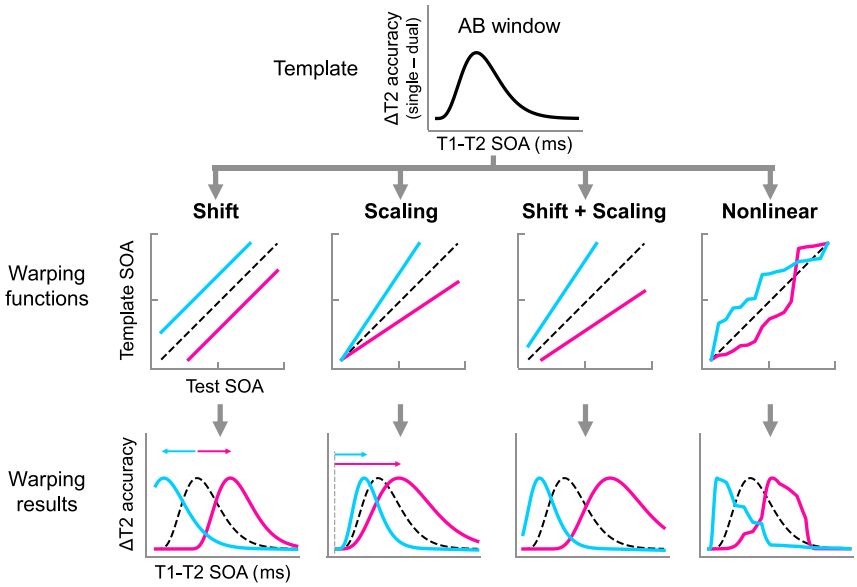

Figure 3. Scheme of time warping analysis

The AB window was defined as the sequence of differences in T2 accuracy between single- and dual-task conditions as a function of the T1–T2 SOA (top row). We used the AB window of humans as a template and transformed the template by the four warping functions (middle row). Each time warping model predicts the AB window in macaques (bottom row). The first column depicts shifting the template (shift model), the second column depicts scaling the template (scaling model), the third column depicts scaling and shifting the template (mixed model), and the fourth column depicts nonuniformly stretching or compressing the template using the DTW algorithm (nonlinear model).

accuracy at the shortest SOA (50 ms) and that at the SOA with the lowest accuracy (300 ms). *t*-Tests revealed that the accuracy was higher when the SOA was 50 ms than when it was 300 ms ($t(83) = 2.40$, $p = 0.019$, $d = 0.51$), indicating lag-1 sparing.

For a direct comparison between macaque and human ABs, we conducted experiments on human subjects using the same task and same trial sequence as those used for macaques (Figure 1). The results showed that the T2 accuracy for the dual task exhibited a U-shaped pattern (Figure 2B, see Figure S2 for the signal detection theory measures). *t*-Tests with Bonferroni corrections revealed significantly lower T2 accuracy in the dual task than in the single task for 50–450 ms of SOA ($p < 0.05$; see Table S2 for statistics). To examine the presence of lag-1 sparing, *t*-tests were performed on the shortest SOA (50 ms) and the SOA with the lowest T2 accuracy (150 ms). The results showed that the accuracy for 50 ms was significantly higher ($t(15) = 4.68$, $p < 0.001$, $d = 0.84$), indicating lag-1 sparing.

Thus, we used a shared dual-task paradigm for both primate species and obtained robust evidence that AB exists in macaques as well as in humans.

Time warping analysis for mapping the relation between attentional blinks of the two species

The macaque AB was not exactly the same as the human AB. For example, the SOA with the lowest T2 accuracy in the dual task and the last SOA with a significant difference between single and dual tasks were longer in macaques than in humans. We next assessed interspecies differences of AB more systematically. A time warping analysis[14–16] was applied to an AB window defined as the sequence of differences in T2 accuracy between single and dual tasks as a function of the T1–T2 SOA. Figure 3 shows a scheme for the analysis that transforms a template (human AB window) along the time axis (T1–T2 SOA) by a warping function to fit another time sequence (macaque AB window). We focused on four models: three warps based on the AB theory and one dynamic warp outside of the theory.

On the basis of the two-stage theory,[1–6] the temporal window of AB reflects the processing at the late stage. Accordingly, the shift model, which alters the intercept of the warping function, accounts for latency to the prevention from the late stage. The scaling model, which alters the slope of the warping function, accounts for the processing speed in the late stage. The mixed model with shift and scaling accounts for both the latency and speed of the late stage. The fourth model uses the dynamic time warping (DTW) algorithm,[14,16] which compresses and stretches a template irrespective of AB theory.

The model parameters such as the shift magnitude and scale factor were determined to minimize the residual error between the warping result (warped human AB window) and the observed data (macaque AB window) at all SOAs (STAR Methods). To evaluate model performance in terms of how well each model can predict the observed data and avoid overfitting, leave-one-out cross-validation (LOOCV) was employed. Figure 4A shows a comparison of root-mean-squared errors (RMSEs) determined by LOOCV for the four models. The results show that the interspecies difference of AB was explained best by the scaling model (Figures 4B and S3). We also applied the scaling model to individual human ABs and found that the scale factor computed from every human participant was lower than that computed from each of the two macaques (Figure 4C). This finding confirms that the interspecies difference of AB was distinct from the individual differences within human ABs.

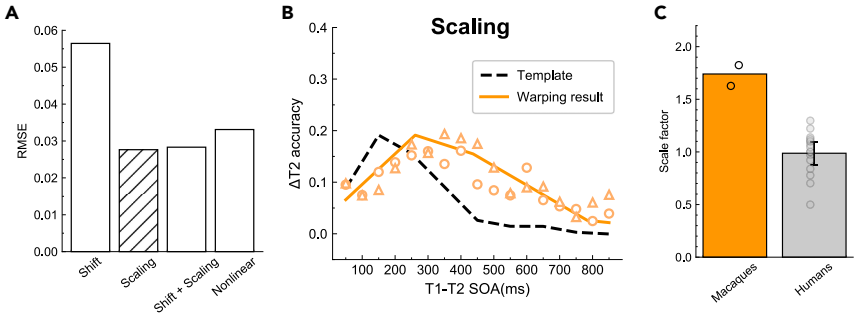

Figure 4. Modeling results on interspecies difference in attentional blink

(A) Comparison of root-mean-square errors (RMSEs) by leave-one-out cross-validation (LOOCV) for the four models. The hatched bar indicates the smallest RMSE.

(B) The warping result in the scaling model. A dashed line indicates the AB window in humans (template). A solid line indicates the predicted AB window in macaques (warping result). Circles and triangles represent the observed data of macaque 1 and macaque 2, respectively.

(C) Comparison of estimated parameters from macaques (orange) and humans (gray) in the scaling model. Each point is the scale factor for each macaque or each human participant. The error bar for humans represents 95% confidence interval of mean. See also Figures S3 and S4.

DISCUSSION

We first established a nonhuman primate model of rigorous AB using a dual-task paradigm shared in macaques and humans (Figure 1). A previous study indirectly suggested an AB in macaques using a delayed-match-to-sample (DMS) task.[8] However, whether the observed behaviors indicated a true AB is questionable. The key feature of AB is that subjects are often unaware of the second target (T2) only when they attend to the first target (T1) in rapid successive visual events. The aforementioned previous study[8] did not verify the key feature of AB because, in the DMS task, which of sample (T1) or test (T2) stimuli the macaques failed to recognize was unclear. By contrast, the current study for macaques ensures the key feature of AB because we set the single-task condition as a control to clarify that attention to T1 induces a deficit of T2 detection in the dual task. As a result, we found that the macaques exhibited a U-shaped psychometric function, similar to the function observed in human AB (Figure 2).

We also observed a difference in the temporal window of AB between macaques and humans, which suggests that temporal processing in AB changed during primate evolution. Time warping analysis[14–16] quantified such an interspecies difference and revealed the temporal structure. As shown in Figures 3, 4A, and 4B, an interspecies difference was explained well by the scaling model. Although the mixed model with shift and scaling achieved almost equal performance, the scaling-only model was sufficient. In relation to a two-stage account for AB,[1–6] the scaling model indicates that the change between macaque and human ABs occurred only at the late stage. We also modeled a dynamic time warp because the interspecies difference can potentially be explained outside of AB theory. Although the dynamic time warp enables an elastic change of the template, the model performance became worse than the scaling model. Collectively, scaling is the best and most parsimonious model: the temporal window of macaque AB was linearly stretched from that of human AB. There is another possibility that the scale factor might be related to the T1 task performance of each subject. However, we did not observe such relations between the scale factor and T1 accuracy for each macaque and human (Figures 4C and S4). These results indicate that the interspecies difference in AB window likely reflects an evolutionary change in the processing speed in the late stage of perception.

Time warping modeling,[14–16] which has rarely been used in psychology and cognitive science, would enable us to achieve an organized view for diverse AB modifications. Moreover, nonlinear modeling using the dynamic time warping (DTW) algorithm can potentially capture an unknown structure from a time series in an unsupervised manner.[14,16] Thus, the current scheme based on time warping can be widely applicable to the data even outside of AB studies, leading to new knowledge of relations between psychometric functions obtained under different conditions.

In the case of our experimental results, the factor computed from the scaling model indicates that the processing speed at the late stage is approximately 1.7 times slower in macaques than in humans (Figure 4C). These results contrast with those of previous studies on sensory evoked potentials,[19,20] where the response latencies of the early phase were longer in humans than in macaques. The early sensory responses within 150 ms have been considered to reflect pre-attentive, unconscious processing,[21] whereas a late evoked potential is likely related to conscious awareness including AB.[21–23] Our results also contrast with those related to another example of invisibility due to forward and backward masking,[24,25] where the time course of the masking effects in macaques and humans was found to be approximately the same. Many theories propose that forward and backward masking are based on the sensory process at lower levels,[26,27] whereas AB is induced by the cognitive process at higher levels.[28,29] The AB duration is assumed to depend on the speed of the later stage, in which visual information is routed to conscious awareness. A recent study estimated the duration of AB in human infants using an eye-tracking paradigm and found that the AB duration shortened across ages.[30] The authors claimed that the acceleration of information processing during infancy is largely due to cortical myelination.[30] In the current study, both the macaques and humans are adults, and their myelinations are mature.[31–33] Thus, these results suggest that the efficiency of the late processing stage increases not only with development but also with primate evolution. This

view is consistent with several studies indicating that AB is involved in the higher-order brain areas such as the parietal and frontal areas,[22,34,35] which expand with development and evolution.[36,37]

The reverse side of the temporal scaling between macaque and human ABs suggests that a scale-invariant mechanism in AB is inherited through primate evolution. We observed that both species showed AB only in the dual-task condition, not in the single-task condition, indicating a common biological constraint for visual awareness. Several studies have shown the cortical bases of AB in humans using functional magnetic resonance imaging (fMRI), electro- and magneto-encephalography (EEG/MEG) techniques.[22,34,35,38–40] However, the neural circuits or dynamics that determine the AB at fine spatial and temporal resolution remain unclear. Moreover, theoretical studies have proposed that subcortical regions such as the thalamus and brainstem are also involved in AB.[5,41,42] Given the advanced technologies of neuroscience that can be applied to animals in combination with theory and psychophysics, our nonhuman primate AB model might be pivotal in gaining a more granular understanding of the biological mechanisms for visual awareness, especially the temporal aspects.[43–45]

Limitations of the study

First, the current results show that an inaccessible time to visual awareness was longer in macaques than in humans. However, the same finding cannot be generalized for perceptual awareness because an animal model of AB for the other sensory modalities (e.g., auditory AB) has not been established. Second, the limited sample size hinders the generalizability of our findings. Specifically, whether the influence of sex, gender, or both on attentional blink exists needs to be tested in future experiments with larger sample size and sex/gender-balanced sampling. Finally, on the basis of the previous EEG studies in human AB, which have indicated that especially P3b, the late evoked potential, is involved in visual AB,[22] the interspecies difference in our study suggests that the latency and/or duration of late evoked potentials such as the P3b component might be longer in macaques than in humans, even though the latency of early evoked potentials is shorter in macaques, as shown by Itoh et al.[19] However, this possibility could not be explored in our behavioral experiments. We would like to clarify this issue by taking a neurophysiological approach to the non-human primate model of AB in a future study.

STAR★METHODS

Detailed methods are provided in the online version of this paper and include the following:

- KEY RESOURCES TABLE
- RESOURCE AVAILABILITY
  - Lead contact
  - Materials availability
  - Data and code availability
- EXPERIMENTAL MODEL AND STUDY PARTICIPANT DETAILS
  - Macaque subjects
  - Human participants
- METHOD DETAILS
  - Apparatus
  - Stimuli
  - Design and procedure
- QUANTIFICATION AND STATISTICAL ANALYSIS
  - Time warping analysis

SUPPLEMENTAL INFORMATION

Supplemental information can be found online at https://doi.org/10.1016/j.isci.2023.108208.

ACKNOWLEDGMENTS

We thank S. Funahashi and J. Saiki for valuable advice on the experiments; A.Tanaka, K. Misawa and K. Kato for critical discussions; K. Yokosaka and A. Maeda for training animals and technical help. This work was supported in part by Grant-in-Aids for Scientific Research (A), KAKENHI JP21H04423 from Ministry of Education, Culture, Sports, Science and Technology and Core Research for Evolutional Science and Technology (18071867) from Japan Science and Technology Agency (all to Y.K.).

AUTHOR CONTRIBUTIONS

Conceptualization, Y.K.; methodology, K.C., A.K. and Y.K.; investigation, H.T. and K.C.; writing – original draft, K.C.; writing – review & editing, K.C., A.K. and Y.K.; funding acquisition, Y.K.; supervision, Y.K.

DECLARATION OF INTERESTS

The authors declare no competing interests.

INCLUSION AND DIVERSITY

We support inclusive, diverse, and equitable conduct of research.

Received: July 14, 2023
Revised: August 26, 2023
Accepted: October 11, 2023
Published: October 31, 2023

REFERENCES

1. Raymond, J.E., Shapiro, K.L., and Arnell, K.M. (1992). Temporary suppression of visual processing in an RSVP Task: an attentional blink? J. Exp. Psychol. Hum. Percept. Perform. *18*, 849–860.
2. Chun, M.M., and Potter, M.C. (1995). A two-stage model for multiple target detection in rapid serial visual presentation. J. Exp. Psychol. Hum. Percept. Perform. *21*, 109–127.
3. Dux, P.E., and Marois, R. (2009). The attentional blink: A review of data and theory. Percept. Psychophys. *71*, 1683–1700.
4. Martens, S., and Wyble, B. (2010). The attentional blink: Past, present, and future of a blind spot in perceptual awareness. Neurosci. Biobehav. Rev. *34*, 947–957.
5. Dehaene, S., Sergent, C., and Changeux, J.-P. (2003). A neuronal network model linking subjective reports and objective physiological data during conscious perception. Proc. Natl. Acad. Sci. USA *100*, 8520–8525.
6. Wyble, B., Bowman, H., and Nieuwenstein, M. (2009). The Attentional Blink Provides Episodic Distinctiveness: Sparing at a Cost. J. Exp. Psychol. Hum. Percept. Perform. *35*, 787–807.
7. Komura, Y., Tamura, R., Uwano, T., Nishijo, H., Kaga, K., and Ono, T. (2001). Retrospective and prospective coding for predicted reward in the sensory thalamus. Nature *412*, 546–549.
8. Maloney, R.T., Jayakumar, J., Levichkina, E.V., Pigarev, I.N., and Vidyasagar, T.R. (2013). Information processing bottlenecks in macaque posterior parietal cortex: An attentional blink? Exp. Brain Res. *228*, 365–376.
9. Ward, R., Duncan, J., and Shapiro, K. (1996). The slow time-course of visual attention. Cogn. Psychol. *30*, 79–109.
10. Jolicoeur, P. (1998). Modulation of the attentional blink by on-line response selection: Evidence from speeded and unspeeded Task1 decisions. Mem. Cognit. *26*, 1014–1032.
11. Husain, M., Shapiro, K., Martin, J., and Kennard, C. (1997). Abnormal temporal dynamics of visual attention in spatial neglect patients. Nature *385*, 154–156.
12. Lacroix, G.L., Constantinescu, I., Cousineau, D., de Almeida, R.G., Segalowitz, N., and Grünau, M.v. (2005). Attentional blink differences between adolescent dyslexic and normal readers. Brain Cogn. *57*, 115–119.
13. Su, L., Naqui, J., Mata-Contreras, J., Martín, F., Wang, Y., Cheung, E., Bowman, H., and Chan, R. (2015). Temporal perception deficits in schizophrenia: integration is the problem, not deployment of attentions. Sci. Rep. *7*, 1–12.
14. Velichko, V., and Zagoruyko, N. (1970). Automatic recognition of 200 words. Int. J. Man Mach. Stud. *2*, 223–234.
15. Williams, A.H., Poole, B., Maheswaranathan, N., Dhawale, A.K., Fisher, T., Wilson, C.D., Brann, D.H., Trautmann, E.M., Ryu, S., Shusterman, R., et al. (2020). Discovering precise temporal patterns in large-scale neural recordings through robust and interpretable time warping. Neuron *105*, 246–259.e8.
16. Sakoe, H., and Chiba, S. (1978). Dynamic programming algorithm optimization for spoken word recognition. IEEE Trans. Acoust. *26*, 43–49.
17. Visser, T.A.W., Bischof, W.F., and Di Lollo, V. (1999). Attentional switching in spatial and nonspatial domains: Evidence from the attentional blink. Psychol. Bull. *125*, 458–469.
18. Jefferies, L.N., Ghorashi, S., Kawahara, J.I., and Di Lollo, V. (2007). Ignorance is bliss: The role of observer expectation in dynamic spatial tuning of the attentional focus. Percept. Psychophys. *69*, 1162–1174.
19. Itoh, K., Konoike, N., Nejime, M., Iwaoki, H., Igarashi, H., Hirata, S., and Nakamura, K. (2022). Cerebral cortical processing time is elongated in human brain evolution. Sci. Rep. *12*, 1103.
20. Schroeder, C.E., Tenke, C.E., Givre, S.J., Arezzo, J.C., and Vaughan, H.G., Jr. (1991). Striate cortical contribution to the surface-recorded pattern-reversal VEP in the alert monkey. Vis. Res. *31*, 1143–1157.
21. Bekinschtein, T.A., Dehaene, S., Rohaut, B., Tadel, F., Cohen, L., and Naccache, L. (2009). Neural signature of the conscious processing of auditory regularities. Proc. Natl. Acad. Sci. USA *106*, 1672–1677.
22. Sergent, C., Baillet, S., and Dehaene, S. (2005). Timing of the brain events underlying access to consciousness during the attentional blink. Nat. Neurosci. *8*, 1391–1400.
23. Shen, D., Vuvan, D.T., and Alain, C. (2018). Cortical sources of the auditory attentional blink. J. Neurophysiol. *120*, 812–829.
24. Kovács, G., Vogels, R., Orban, G.A., and Sprague, J.M. (1995). Cortical correlate of pattern backward masking. Proc. Natl. Acad. Sci. USA *92*, 5587–5591.
25. Macknik, S.L., and Livingstone, M.S. (1998). Neuronal correlates of visibility and invisibility in the primate visual system. Nat. Neurosci. *1*, 144–149.
26. Kahneman, D. (1968). Method, Findings, and Theory in Studies of Visual Masking. Psychol. Bull. *70*, 404–425.
27. Macknik, S.L., and Martinez-Conde, S. (2004). The spatial and temporal effects of lateral inhibitory networks and their relevance to the visibility of spatiotemporal edges. Neurocomputing *58–60*, 775–782.
28. Breitmeyer, B.G. (2015). Psychophysical "blinding" methods reveal a functional hierarchy of unconscious visual processing. Conscious. Cogn. *35*, 234–250.
29. Kanai, R., Walsh, V., and Tseng, C.H. (2010). Subjective discriminability of invisibility: A framework for distinguishing perceptual and attentional failures of awareness. Conscious. Cogn. *19*, 1045–1057.
30. Hochmann, J.R., and Kouider, S. (2022). Acceleration of information processing en route to perceptual awareness in infancy. Curr. Biol. *32*, 1206–1210.e3.
31. Kovacs-Balint, Z.A., Payne, C., Steele, J., Li, L., Styner, M., Bachevalier, J., and Sanchez, M.M. (2021). Structural development of cortical lobes during the first 6 months of life in infant macaques. Dev. Cogn. Neurosci. *48*, 100906.
32. Gibson, K.R. (1970). Sequence of Myelinization in the Brain of Macaca mulatta (University of California).
33. Kubicki, M., Baxi, M., Pasternak, O., Tang, Y., Karmacharya, S., Chunga, N., Lyall, A.E., Rathi, Y., Eckbo, R., Bouix, S., et al. (2019). Lifespan Trajectories of White Matter Changes in Rhesus Monkeys. Cereb. Cortex *29*, 1584–1593.
34. Marois, R., Chun, M.M., and Gore, J.C. (2000). Neural Correlates of the Attentional Blink. Neuron *28*, 299–308.
35. Kranczioch, C., Debener, S., Schwarzbach, J., Goebel, R., and Engel, A.K. (2005). Neural correlates of conscious perception in the attentional blink. Neuroimage *24*, 704–714.
36. Hill, J., Inder, T., Neil, J., Dierker, D., Harwell, J., and Van Essen, D. (2010). Similar patterns of cortical expansion during human development and evolution. Proc. Natl. Acad. Sci. USA *107*, 13135–13140.
37. Griffa, A., and Van den Heuvel, M.P. (2018). Rich-club neurocircuitry: function, evolution, and vulnerability. Dialogues Clin. Neurosci. *20*, 121–132.
38. Luck, S.J., Vogel, E.K., and Shapiro, K.L. (1996). Word meanings can be accessed but not reported during the attentional blink. Nature *383*, 616–618.
39. Gross, J., Schmitz, F., Schnitzler, I., Kessler, K., Shapiro, K., Hommel, B., and Schnitzler, A. (2004). Modulation of long-range neural synchrony predicts temporal limitations of visual attention in humans. Proc. Natl. Acad. Sci. USA *101*, 13050–13055.
40. Janson, J., and Kranczioch, C. (2011). Good vibrations, bad vibrations: Oscillatory brain activity in the attentional blink. Adv. Cogn. Psychol. *7*, 92–107.
41. Raffone, A., Srinivasan, N., and van Leeuwen, C. (2014). The interplay of attention and consciousness in visual search, attentional blink and working memory consolidation. Philos. Trans. R. Soc. Lond. B Biol. Sci. *369*, 20130215. https://doi.org/10.1098/rstb.2013.0215.
42. Nieuwenhuis, S., Gilzenrat, M.S., Holmes, B.D., and Cohen, J.D. (2005). The role of the locus coeruleus in mediating the attentional blink: A neurocomputational theory. J. Exp. Psychol. Gen. *134*, 291–307.

43. Dehaene, S., and Changeux, J.P. (2011). Experimental and theoretical approaches to conscious processing. Neuron *70*, 200–227.

44. Koch, C., Massimini, M., Boly, M., and Tononi, G. (2016). Neural correlates of consciousness: progress and problems. Nat. Rev. Neurosci. *17*, 307–321.

45. Lamme, V.A.F. (2010). How neuroscience will change our view on consciousness. Cogn. Neurosci. *1*, 204–220.

46. Brainard, D.H. (1997). The Psychophysics Toolbox. Spat. Vis. *10*, 433–436.

47. R Core Team (2022). R: A Language and Environment for Statistical Computing (R Foundation for Statistical Computing).

48. Champely, S. (2020). Pwr: Basic Functions for Power Analysis (Comprehensive R Archive Network).

49. Virtanen, P., Gommers, R., Oliphant, T.E., Haberland, M., Reddy, T., Cournapeau, D., Burovski, E., Peterson, P., Weckesser, W., Bright, J., et al. (2020). SciPy 1.0: fundamental algorithms for scientific computing in Python. Nat. Methods *17*, 261–272.

50. Komura, Y., Nikkuni, A., Hirashima, N., Uetake, T., and Miyamoto, A. (2013). Responses of pulvinar neurons reflect a subject's confidence in visual categorization. Nat. Neurosci. *16*, 749–755.

51. Komura, Y., Tamura, R., Uwano, T., Nishijo, H., and Ono, T. (2005). Auditory thalamus integrates visual inputs into behavioral gains. Nat. Neurosci. *8*, 1203–1209.

52. Macmillan, N.A., and Creelman, C.D. (2004). Detection Theory: A User's Guide, 2nd Edition (Psychology Press).

53. Green, D.M., and Swets, J.A. (1966). Signal Detection Theory and Psychophysics (John Wiley).

STAR★METHODS

KEY RESOURCES TABLE

REAGENT or RESOURCE	SOURCE	IDENTIFIER
Deposited data		
Data and codes for all the figures	This paper Mendeley Data	https://doi.org/10.17632/6hrrnzdsz7.1
Experimental models: Organisms/strains		
Macaque monkey (*Macaca fuscata*)	National BioResource Project, Kawahara Co. Ltd, Japan	N/A
Software and algorithms		
MATLAB R2006a	Mathworks	RRID: SCR_001622
Psychophysics Toolbox v3	Brainard[46]	RRID: SCR_002881
Python	Python Software Foundation	RRID: SCR_008394
R Version 4.2.1	R Core Team[47]	RRID: SCR_001905
R package "pwr"	Champely[48]	https://CRAN.R-project.org/package=pwr
SciPy	Virtanen et al.[49]	RRID: SCR_008058
iRecHS2	Open source	https://staff.aist.go.jp/k.matsuda/eye/

RESOURCE AVAILABILITY

Lead contact

Further information and requests for resources should be directed to and will be fulfilled by the lead contact, Yutaka Komura (komura.yutaka.6a@kyoto-u.ac.jp).

Materials availability

This study did not generate new unique reagents.

Data and code availability

- The analysed data have been deposited at Mendeley Data and are publicly available as the date of publication. DOI is listed in the key resources table.
- All original codes have been deposited at Mendeley Data and are publicly available as the date of publication. DOI is listed in the key resources table.
- Any additional information required to reanalyze the data reported in this paper is available from the lead contact upon reasonable request.

EXPERIMENTAL MODEL AND STUDY PARTICIPANT DETAILS

Macaque subjects

Two healthy adult macaques at 9-11 years of age (*Macaca fuscata*, one male (macaque 1) and one female (macaque 2), weighing 5-8 kg) were used in the experiment. During the experiment, the animals showed no signs of any infections and immunological diseases. Therefore, we did not administer any drugs to them for medication. We used the naïve macaques with no history of any other experiments. Prior to this study, the animals were not involved in any other research or non-research procedures. We minimized the number of macaques used due to the ethics and data similarity. Each macaque was housed in an individual stainless-steel cage with environmental enrichment and provided with access to uncontaminated water and food. The housing area was maintained at 24°C ± 4°C, 50% ± 20% relative humidity, and with a 12 h:12 h light/dark cycle. The cages and housing area were regularly cleaned and sanitized. Considering nutritional balance, the macaques were fed certified primate diets (PS-A, Oriental Yeast Co., Ltd.) and supplemented with fresh fruits and vegetables. We conducted husbandry trainings to keep the macaques healthy. Body weight and water intake were measured daily to ensure their health conditions. The experiments were conducted during the light cycle. Details of procedures used in the present study are similar to those previously described.[50,51] During the experimental sessions, the macaques were seated in a primate chair and their heads were immobilized with the head holder, thereby allowing the macaques to face the CRT display squarely. The head holder was implanted into the macaques under anesthesia and sterile surgical

conditions. All experimental procedures in macaques were approved by the Animal Research Committee at the Graduate School of Human and Environmental Studies, Kyoto University, and performed following the NIH Guide for the Care and Use of Laboratory Animals.

Human participants

Sixteen Japanese adults (five females; minimum = 19 years, maximum = 33 years, mean = 24.3 ± 4.6) participated in the experiment. All had normal or corrected-to-normal visual acuity. The sample size was decided on the basis of the previous studies of attentional blink.[2,3] Participants received a full explanation and signed an informed consent form to participate in the experiment. During the experiment, participants performed the task in a dark room with their heads immobile by a chin-rest. Because the experiment was conceptualized as within-subjects design, all participants completed all conditions. All procedures in humans were performed following the principles of the Declaration of Helsinki and approved by the Human Studies Committee of the Graduate School of Human and Environmental Studies at Kyoto University. The influence of sex, gender, or both on the data was not specifically tested in this study.

METHOD DETAILS

Apparatus

For macaques, under the control of REX (a QNX-based real-time experiment management system) stimuli were presented by ViSaGe (Cambridge Research Systems) on a CRT display (21-inch; 1024 × 768 pixel resolution; refresh rate 100 Hz). For humans, stimulus creation and experimental control were performed in MATLAB R2006a (Math Works) using Psychtoolbox,[46] and stimuli were presented on a CRT display (21-inch, 1024 × 768 pixel resolution; Refresh rate 100 Hz). Each display was gamma-corrected using a colorimeter (ColorCAL MKII, Cambridge Research Systems) and was placed 57 cm from the observers. The eye position of the macaques was monitored using iRecHS2 software with an infrared high-frame-rate digital camera (FLIR, GS3-U3-32S4M-C).

Stimuli

Throughout the experiment, each stimulus was presented on a uniform gray background (15 cd m^{-2}). Each trial consisted of a rapid sequential visual presentation (RSVP) with two embedded targets (T1 and T2) and masks following T2: The first target (T1) was a sinusoidal grating with horizontal or vertical orientation (spatial frequency 2.0 cpd; contrast 100%; size 2.0 ° × 2.0 °); the second target (T2) was a white disk (50 cd m^{-2}; diameter 1.0–1.2° and 0.8–1.2° for macaques and humans, respectively). The mask stimulus was a mosaic pattern of 6 × 6 grids, with 18 random grids per mask consisting of white (50 cd m^{-2}) and the remaining 18 grids the same gray (15 cd m^{-2}) as the background, with one side the same size as the T2 diameter.

Each trial began with a colored gazing cross (task cue: 5 cd m^{-2}; 0.5 ° × 0.5 °) presented in the center of the display for 300 ms; the color of the task cue (blue or red) depended on the task condition performed by the subject. After the task cue, the color of the gazing cross changed to white (50 cd m^{-2}) and continued to be presented in the center of the display during the subsequent stimulus presentation. Following the fixation period of 400–700 ms, T1 appeared at the center of the display for 50 ms. Intervening a variable lag after T1 onset (T1–T2 SOA; 17 points [50:50:850 ms] for macaques, and 9 points [50:100:850 ms] for humans), T2 and two masks were presented for 20 ms each, separated by a blank interval of 80 ms at a left parafoveal location on the display ($-6.5° \leq x \leq -3.5°$, $-1.0° \leq y \leq 1.0°$) for neurophysiological investigations in our future study. T2 was presented in one-half of all the trials, and the size and position of T2 were adjusted for each participant (see design and procedure section); the position was determined with a jitter of ±1.0° vertically and horizontally for each trial. After a 500–800 ms delay after the second mask presentation, the central gaze cross changed to the blue response cue (5 cd m^{-2}; diameter 0.5°) cueing the T2 report (Q2). In the single-task condition, in which only T2 detection was required, the trial ended at this point. In the dual-task condition, in which T1 identification in addition to T2 detection was required, the color of the response cue changed to red as a cue for the T1 reporting (Q1) after Q2.

Design and procedure

Macaques

Each trial was initiated by the macaque gripping the center bar (home bar) and looking at the gazing cross. While the stimulus sequence was presented, the macaque had to keep looking at the gazing cross, Q2, or Q1. If the macaque blinked or looked outside the 3° square of the center of the display (fixation break), the ongoing trial was terminated at that point and the next trial began after the intertrial interval, without any reward.

The macaques performed two types of tasks—a single-task condition and a dua-task condition—and each condition was divided by blocks. In the single task, the macaques were required to detect T2 presented in one-half of all the trials; if T2 was present, the macaques were required to release and then re-grip the home bar within 750 ms in Q2. In the dual task, the macaques were required to detect T2 while determining whether T1 was a horizontal or vertical grating; after reporting the presence of T2, as in the single-task condition, the macaques had to touch the upper-left bar if T1 was a horizontal grating or the upper-right bar if it was a vertical grating within 850 ms in Q1. For macaques, correct responses were rewarded with a drop of water or juice after answering Q2 in the single task or after answering both Q2 and Q1 in the dual task. In the dual task, reward size was more than twice as much as in the single task to motivate the macaques. The intertrial interval was 1500–2000 ms. In total, we collected 68885 trials (23849 trials in the single-task condition and 45036 trials in the dual-task condition) from the two macaques in 355 experimental sessions (169 sessions for macaque 1 and 186 sessions for macaque 2).

Humans

The task for each trial was the same as for the macaques. In reporting the T2 presence, participants were required to click on the circle with a diameter of 4° presented at the bottom of the display within 1500 ms in Q2. In reporting the T1 orientation, two circles, each with a diameter of 4°, on both the left and right at the top of the display were presented during the Q1 period and participants were instructed to click on the upper-left circle if T1 was horizontal and on the upper-right circle if it was vertical within 2000 ms in Q1. Participants were instructed to look at the gazing cross in the center of the display while the stimuli were presented. The intertrial interval was 1000–1500 ms. Each participant completed multiple practice blocks consisting of 20 trials per block for both the single and dual tasks prior to the start of the experiment. During the first practice block, the experimenter provided verbal feedback on the correctness of the target report. During the practice block, the size and position of the T2 were adjusted so that each participant's T2 detection accuracy for long SOAs (500–850 ms) in the single task was greater than 95%; this parameter was fixed in a subsequent experiment. The single- and dual-task conditions were conducted in separate blocks. Each block consisted of 144 trials, with three blocks for the single task and six blocks for the dual task. During the single task, participants were instructed to only perform T2 detection, with no attention to T1. No feedback was given to human participants during the experiment blocks. Between each block, participants were given a self-paced break.

QUANTIFICATION AND STATISTICAL ANALYSIS

The analyses in this study were performed using Python (version 3.11.1). For statistical tests and estimations of effect size, R[47] (version 4.2.1) with the pwr[48] library was used. For all *t*-tests, a two-tailed test was used. Multiple comparisons were corrected by the Bonferroni method with an α-level of .05. In the dual-task condition, only trials in which subjects responded correctly to the T1 discrimination were included in the analysis. On the basis of signal detection theory,[52,53] we also computed sensitivity (d') and bias (c) for the T2 task performance.

Time warping analysis

To capture a commonality and difference between macaque and human ABs systematically, we introduced a time warping method.[14–16] First, we defined an AB window as the sequence of difference in T2 accuracy between the single and dual tasks as a function of the T1–T2 SOA. Second, we used the AB window of humans as a template ($f_{template}$) and transformed the template by each of the warping functions to match the AB window of macaques. In this modelling except for the nonlinear model (see below), the model parameters were determined to minimize the residual error between the warping result (warped template of human AB window: f_{result}) and observed data (macaque AB window) at all SOAs using scipy.optimize.fmin.[49] The each warping result (f_{result}) was derived from following equations.

$$f_{result}(x) = f_{template}(x - \Delta x) \qquad shift$$

$$f_{result}(x) = f_{template}\left(\frac{x}{c_x}\right) \qquad scaling$$

$$f_{result}(x) = f_{template}\left(\frac{x}{c_x} - \Delta x\right) \qquad shift + scaling$$

$$f_{result}(x) = f_{template}(N(x)) \qquad nonlinear$$

Here, x is the T1-T2 SOA and Δx (shift magnitude) and c_x (scale factor) are parameters for warping. The N function in the nonlinear model is defined by the warping path (W^*) in the Dynamic Time Warping (DTW) algorithm.[14,16]

The DTW changes the shape of the time axes so that the two time series are as similar as possible. In our case, two time series are the AB window of humans ($f_{template}$) and the AB window mean of macaques (f_{data}). We performed the DTW with linear interpolation to the AB window of humans to align the number of SOAs with those of macaques. To obtain W^*, the DTW begins by defining W, which is the sequence of two components ($w_{data}, w_{template}$). $W(k)$ ($k = 1,2,\ldots,K$) is the pair of SOAs that indicates which the SOA of template ($w_{template}(k)$) warps to which the SOA of the observed data ($w_{data}(k)$):

$$W(k) = \left(w_{data}(k), w_{template}(k)\right) \text{ with}$$

$$w_{data}(k) \text{ and } w_{template}(k) \in \{50, 100, \ldots, 850\}.$$

W is under the following constraints:

$$W(1) = \left(w_{data}(1), w_{template}(1)\right) = (50, 50),$$

$$W(K) = \left(w_{data}(K), w_{template}(K)\right) = (850, 850),$$

$$W(k+1) = \begin{cases} (w_{data}(k), w_{template}(k)+50), \\ (w_{data}(k)+50, w_{template}(k)+50), \\ \text{or } (w_{data}(k)+50, w_{template}(k)). \end{cases}$$

Therefore, W is an arbitrary path drawing the upward-sloping graph (see the graph of nonlinear warping function in Figure 3). To find the warping path which best transforms the template ($f_{template}$) to the observed data (f_{data}), we calculated the difference between two functions as follows:

$$d(W) = d(w_{data}, w_{template}) = \sum_{k=1}^{K} \left\| f_{data}(w_{data}(k)) - f_{template}(w_{template}(k)) \right\|.$$

W^* is the path which minimizes the difference:

$$W^* = \underset{W}{\operatorname{argmin}} d(W).$$

Now, nonlinear warping function $N(x)$ is defined by using $W^*(k) = (w^*_{data}(k), w^*_{template}(k))$:

$$N(x) = w^*_{template}(k; w^*_{data}(k) = x).$$

If multiple SOAs of the template corresponded to an SOA of the observed data, we used the average of the AB windows of the template at those SOAs.

Third, we evaluated model performance by leave-one-out cross-validation (LOOCV). In the LOOCV, one of the data from either macaque in an SOA was first removed (test data) and the remaining data (training set) were used to estimate the parameters (Δx, c_x) or the warping path (W^*). Based on the estimation, we quantified the model performance by the squared error between the model prediction and test data. This process was repeated for all possible combinations, and the root-mean-squared error (RMSE) was calculated for each model. Finally, the model with the lowest RMSE by LOOCV was selected as the best model describing the relationship between macaque and human ABs.